*Materials and Structures/Matériaux et Constructions*, Supplement March 1997, pp 54-62

LECTURE DELIVERED BY THE ROBERT L'HERMITE MEDALLIST FOR 1996

# Strain rate effects in concrete structures: the LCPC experience

*Dr. P. Rossi*

*Laboratoire Central des Ponts et Chaussées, 58 bd. Lefèbvre, Paris F 75732, France.*

## ABSTRACT

This paper presents, first, a synthesis of the research work carried out at LCPC on the dynamic behaviour of concrete structures, and second, the studies which remain to be performed in response to professional needs.

The main advances of this research can be summarized as follows:

– For strain rates less or equal to 1 $s^{-1}$, an increase in material strength is related to viscous phenomena due to the presence of free water in the nanopores of concrete hydrates. This increase is independent of the water/cement ratio of the concrete. For strain rates equal to or greater than 10 $s^{-1}$, inertia forces are mainly responsable for increasing strength.

– Two numerical modellings are being implemented in the finite-element code CESAR-LCPC: the first is a visco-elastoplastic degrading model with viscous hardening; the second is a discrete probabilistic viscous cracking model. These models take into account the physical mechanisms observed and analyzed during the experimental studies.

Further experimental and theoretical studies of the dynamic behaviour of the rebar/concrete interface appear as a priority for the future.

## RÉSUMÉ

*Cet article présente, d'une part, une synthèse des travaux réalisés au Laboratoire Central des Ponts et Chaussées sur le comportement dynamique des structures en béton, et d'autre part, une liste, non exhaustive, des recherches qu'il reste à mener dans le domaine pour répondre aux besoins des professionnels.*

*Les principales connaissances acquises, ainsi que les avancées constatées lors de ces travaux peuvent se résumer ainsi :*

*– C'est la présence d'eau libre à l'échelle des hydrates du béton qui induit des augmentations de résistance, indépendantes du rapport eau/ciment du béton, pour des vitesses de déformation inférieures ou égales à 1 $s^{-1}$. Pour des vitesses de déformation supérieures ou égales à 10 $s^{-1}$, ce sont principalement les effets d'inertie qui sont à l'origine des augmentations de résistance.*

*– Deux modèles numériques relatifs au comportement dynamique du béton ont été développés et intégrés dans le code aux éléments finis CESAR-LCPC : le premier est un modèle visco-élastoplastique avec écrouissage visqueux, alors que le second est un modèle probabiliste de fissuration discrète avec prise en compte de la viscosité du matériau. Ces deux modèles intègrent les mécanismes physiques mis en évidence lors des études expérimentales.*

*L'étude expérimentale et théorique du comportement en dynamique de l'interface acier-béton est considérée comme prioritaire pour les années à venir.*

## 1. INTRODUCTION

The Laboratoire Central des Ponts et Chaussées (LCPC) has been working, since about 1990, on the dynamic behaviour of concrete, both on the level of the material and on the structural level [1-9]. One of the main results of this research is that the observed effects of loading rate on the mechanical behaviour of concrete depend mainly, within a certain rate range, on the presence of free water in the nanopores of the hydrates of concrete. A hypothesis has been advanced concerning the physical mechanism underlying the effects of loading rate, a mechanism which is related to the Stéfan effect and proportional to the viscosity of the water.

This article attempts to synthesize the various work and findings of LCPC concerning the strain rate effects in concrete structures, and to evaluate the experimental and theoretical investigations which remain to be performed in the future to better analyse and model the dynamic behaviour of concrete structures. Thus, it is composed of four parts:

– some remarks concerning the physical mechanisms, and in

*Editorial note*

*Pierre Rossi is working at the Laboratoire Central des Ponts et Chaussées, a French RILEM Titular Member. Pierre Rossi was a member of RILEM Technical Committee 90 FMC on Fracture Mechanics of Concrete; he is still active as a member of the Editorial Group of this committee. He is also participating in the work of the recently set-up Technical Committee TDF on Test and Design methods for steel Fibre reinforced concrete. Dr. Rossi was awarded the Robert l'Hermite Medal for 1996 at the last meeting of the RILEM General Council in Garston, UK, on 26 September 1996. This paper is the final version of the lecture delivered by the author on this occasion.*

0025-5432/97 

particular how the Stéfan effect, the cracking process and the inertia forces participate together in the dynamic behaviour of a specimen subjected to a uniaxial tensile test (after [10]),
– an analysis of the transition from the material behaviour to the structural behaviour,
– the LCPC modelling strategy for dynamic behaviour of concretes and concrete structures,
– an overview of the principal experimental and theoretical work which remains to be done.

# 2. PHYSICAL MECHANISMS INVOLVED IN STRAIN RATE EFFECTS IN CONCRETE

## 2.1 The Stéfan effect

This effect can be summarized as follows: when a thin film of a viscous liquid is trapped between two perfectly plane plates that are moved apart at a displacement rate $\dot{h}$, the film exerts a return force on the plates that is proportional to the velocity of separation. This mechanism is reflected by the following equation:

$$F = \frac{3\eta V^2}{2\pi h^5} \cdot \dot{h} \qquad (1)$$

where:
F is the return force,
$\eta$ is the viscosity of the liquid,
h is the initial distance between the two plates,
$\dot{h}$ is the velocity of separation of the two plates ($\dot{h} > 0$),
V is the volume of the liquid.

If it is assumed that the presence of free water in the concrete pores underlies a mechanism of this type when the solid matrix (here regarded as a network of plates) is subjected to tensile strains, it can be understood why loading rate effects are large in wet concretes and very small in dry concretes (Fig. 1). Moreover, it has been shown [3] that the absolute increase of the tensile strength and of Young's modulus due to rate effects is independent of the w/c ratio (Fig. 2). Knowing that the diameter of the micropores of the hydrates is, unlike that of the capillaries, independent of the w/c ratio of the concrete, it is assumed that the micropores of the hydrates play a preponderant role in strain rate effects.

## 2.2 The cracking process in concrete subjected to uniaxial tensile static loading

The process of cracking in a concrete specimen under a uniaxial tensile force can be described by three successive stages as the force increases:

***1. First stage: diffuse microcracking***

During this stage, the initial microcracks (due to the shrinkage of the cement paste, blocked by the aggregates [11]) propagate and new microcracks form in the zones of lowest strength (paste-aggregate bond, for example), or in those zones where the local tensile stresses are high (this is related to the fact that the aggregates and the cement paste have different mechanical characteristics). This microcracking is diffuse, in other words, randomly distributed throughout the volume of the specimen.

***2. Second stage: localization of microcracking***

As they propagate, the microcracks created during the first stage "branch" to form one or more macrocracks. This is the phenomenon of crack localization in particular zones of the specimen. The creation of macrocracks constitutes the start of the third stage.

***3. Third stage:*** propagation of one of the macrocracks created during the previous stage, leading to failure of the specimen.

It must be noted that the notions of microcrack and macrocrack are relative, defined as follows depending on the volume of the specimen:

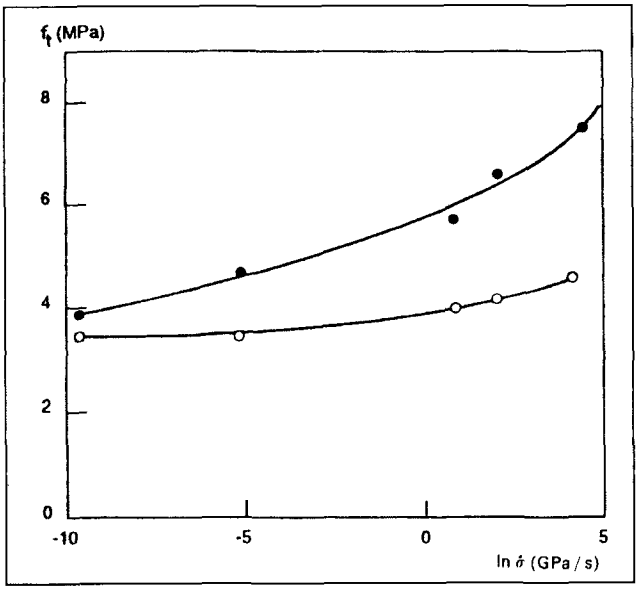


Fig. 1 – Influence of the presence of free water on strain rate effects in concrete: ○, dry specimen; ●, wet specimen.

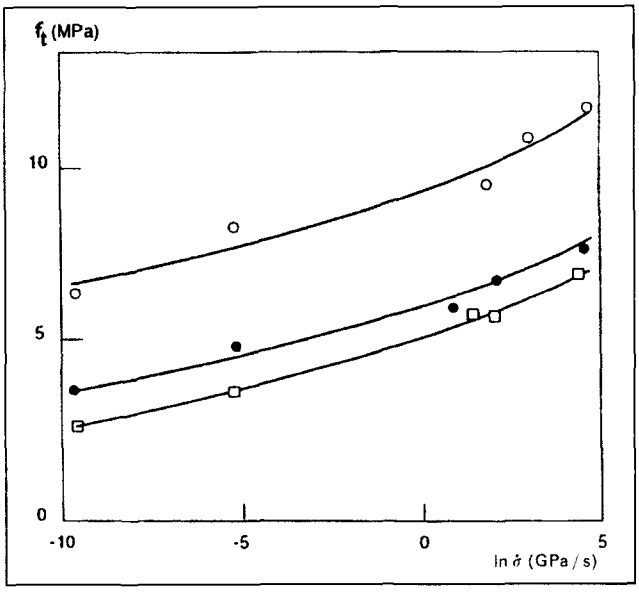


Fig. 2 – Influence of w/c ratio on strain rate effects in concrete: ○, 0.3; ●, 0.5; □, 0.7 (After [3]).

**microcrack**: a crack that is very small with respect to the volume of the specimen,
**macrocrack**: a crack of which the size is not negligible with respect to the volume of the specimen and larger than the maximum aggregate size of the concrete.

When the mechanical behaviour of the specimen corresponding to the different stages of cracking is considered, the following is found if the test is performed at an imposed displacement rate [12]:
– during the stage of diffuse microcracking, the force applied to the specimen increases monotonically with the displacement and is very nearly proportional to the displacement;
– when the microcracking localizes to form macrocracks, the force increases up to a maximum value, but there is a slight non-linearity just before the peak load on the force-displacement curve;
– finally, the propagation of a macrocrack leading to failure of the specimen coincides with a decrease in the force as the displacement increases. This is called "post-peak" or "softening" behaviour.

The mechanical behaviour before crack localization, which coincides with the peak load, can be regarded as intrinsic to the material because, since the cracks are small with respect to the volume of the specimen, statistically homogeneous stresses and strains can be defined (this is one condition for the existence of a constitutive relation for a heterogeneous material).

After localization, on the other hand, since these cracks are no longer assumed to be small with respect to the volume of the specimen, statistically homogeneous stresses and strains can no longer be defined, and therefore the only relation is that between the force and the displacement, which are global parameters. The behaviour is then structural.

This transition from a material behaviour to a structural behaviour during a uniaxial tensile test can also be understood as follows:
– before localization, the spatial distribution of the microcracks could be different (virtual permutations are possible), but would leave the relation between the force and the displacement practically unchanged; therefore, it can be deduced that there is a stress/strain relation intrinsic to the material;
– after localization, if the same is applied to the macrocracks, the relation will depend significantly on the positions of the macrocracks in the specimen, which is typical structural behaviour.

## 2.3 The cracking process in concrete subjected to uniaxial tensile dynamic loading

When the loading rate is increased in a uniaxial tensile test, the Stéfan effect acts as follows on the cracking process (within the context of our hypotheses):

1. Before localization, the Stéfan effect can have two consequences:
– delaying the creation of the microcracks;
– delaying the propagation of the initial microcracks.

These two actions both delay localization of microcracks (and thus increase the peak load) and increase the apparent Young's modulus of the concrete.

It must be reported here that the Stéfan effect has a greater influence on the peak load than on Young's modulus [4] because, in the case of the latter parameter, the aggregates, which play an important role, are not subject to the Stéfan effect, unless they are porous and wet.

2. After localization, the Stéfan effect tends to oppose the propagation of the macrocrack.

In parallel to the Stéfan effect, inertia forces can no longer be neglected when the loading and strain rates generated by a dynamic loading reach high values.

Before the stage of crack localization, these inertia forces can act in two different ways during dynamic loading:
– first, during the acceleration resulting from the imposed loading,
– then, during the creation and propagation of the microcracks, because a material point at the surface of one of the edges of a microcrack that has just been created, or propagated, changes very rapidly from a speed V1 (before cracking) to a speed V2 >> V1 (after cracking).

These forces of inertia have the consequence of opposing both the onset of microcracks and their propagation, thereby delaying microcrack localization. Inertia also acts after the stage of crack localization, opposing the propagation of the macrocrack (the same mechanism as for microcracks).

It is clear that, even though they can act simultaneously, the Stéfan effect and inertia forces are activated with different intensities according to the loading rate imposed on the specimen. A simple model, developed by Bailly [13], has been used for the effects of loading rate on the compressive behaviour of concrete (the criterion of failure, in this model, is that of critical extension). This model, fitted to experimental results, seems to indicate that, at strain rates smaller than a critical value of about 1 $s^{-1}$, the inertia forces are negligible with respect to viscous effects, and that, at rates greater than or equal to this strain rate, the inertia forces are no longer negligible at all, becoming preponderant above a strain rate of approximately 10 $s^{-1}$. However, considering the few experimental results [14, 15] taken from the literature on the effect of the loading rate in concrete subjected to uniaxial tension, it is found that the tensile strength-log of the strain rate relation departs from linearity (a sudden increase in strength is observed) at threshold strain rates close to 1 $s^{-1}$.

Considering the definitions given previously for behaviour at the material level and at the structural level, it is quite possible that the forces of inertia activated by the propagation of the macrocrack (after the localization stage) are sufficient, at some strain rates, to increase the macroscopic tensile strength. In other words, because of the inertia, it may be that when the loading rate is very high, the maximum load does not coincide with the localization of the microcracking, and consequently the jump in tensile strength observed at a strain rate of approximately 1 $s^{-1}$ is only a structural effect.

## 3. FROM THE MATERIAL TO THE STRUCTURE

In a previous paper [4], we discussed the fact that it is not obvious to directly deduce the performance of a concrete structure submitted to an impact loading solely on the basis of knowledge of the dynamic behaviour of the concrete of which this structure is made.

We related this difficulty to the possible change of mechanism of failure of the structure due to the loading rate, the boundary conditions, and the type of concrete.

The physical explanation we proposed was the following:

When a volume of material is loaded very rapidly, there is an acceleration of the material points in the vicinity of the points of application of the forces. This acceleration occurs in a very short time during which very large stress peaks appear. This phase is then followed by a longer transient regime that affects all the particles of the volume of material, and finally, sometimes (this depends on the problem), by a steady state. The greater the Young's modulus of the material, the larger these stress peaks will be. So, there exist mechanisms on the scale of the structure that are not taken into consideration on the scale of the material.

This very brief phase of acceleration of some of the material points in the vicinity of the zone of application of the dynamic loading is regarded as a phenomenon that can participate in the change of mechanism of failure of a structure when it is subjected to faster and faster loadings. In fact, depending on the type of structure and the type of loading, these stress peaks may be tensile peaks leading to the onset of local cracks that propagate and cause failure of the structure either in shear or by punching (depending on the boundary conditions). If the global mechanism of failure of the structure under dynamic loading is a mechanism of bending failure, there will then be competition between this global mechanism (cracking due to bending) and the local mechanism described above (cracks created by the acceleration of the material points); if, on the other hand, the main mechanism of failure is a mechanism of shear failure, it is then obvious that it will be this mechanism that will actually appear. Depending on the type of structure, the type of loading, the Young's modulus of the concrete, and the quality of the bond between concrete and the reinforcement (in the case of reinforced concrete structures), the transition from one mechanism to the other will occur at very different loading rates.

Studying strain rate effects by performing tests simultaneously at the scale of the material and at the scale of the structure, F. Toutlemonde [16] analyzed in detail this problem of change of failure mechanisms.

## 4. MODELLING STRATEGY OF CONCRETE AND CONCRETE STRUCTURES

Two different objectives can be aimed for when mechanical modellings of the dynamic behaviour of concrete are developed:

- the first is related to the design codes, for which it is important to know and to take into account the evolution of the mechanical characteristics of a concrete as a function of the stress or the strain rates in order to design a structure submitted to dynamic loading,
- the second is related to developing constitutive relations of dynamic behaviour of concrete for finite element analysis.

### 4.1. Design code approach

Concerning the first objective, we first proposed [4] the following relations:

$$f_{tdyn.} = f_{tsta.} + \Phi \quad (2)$$

$$E_{dyn.} = E_{sta.} + \varnothing \quad (3)$$

where:

- $f_{tdyn.}$ and $E_{dyn.}$ are respectively the dynamic tensile strength and the dynamic Young's modulus,
- $f_{tsta.}$ and $E_{sta.}$, the static tensile strength and the static Young's modulus related to a reference loading rate of 0.05 MPa/s,
- and $\Phi$ and $\varnothing$, two functions depending on $\ln(\dot{\sigma}_{dyn.}/\dot{\sigma}_{sta.})$, independent of w/c to take into account the experimental results, but possibly dependent on concrete mix design parameters such as the volume of cement paste and the volume of the maximum aggregate size.

Improving this approach, F. Toutlemonde [9, 16] proposed and validated two "types" of relations, for the range $5.\ 10^{-5}$ GPa/s $< \dot{\sigma} <$ 50 GPa/s:

***First series of relations:***

$$f_{tdyn.} = f_{tsta.} + 0.7 \log(\dot{\sigma}_{dyn.}/\dot{\sigma}_{stat.}) \cdot \varphi(H) \quad (4)$$

$$f_{cdyn.} = f_{csta.} + 4.5 \log(\dot{\sigma}_{dyn.}/\dot{\sigma}_{stat.}) \cdot \varphi(H) \quad (5)$$

$$E_{dyn.} = E_{sta.} + 0.9 \log(\dot{\sigma}_{dyn.}/\dot{\sigma}_{stat.}) \cdot \varphi(H) \quad (6)$$

where $f_{cdyn.}$ and $f_{csta.}$ are respectively the dynamic and the static compressive strength, $f_t$ and $f_c$ in MPa, E in GPa, $\varphi(H) = 1$ for wet concrete and $\varphi(H) = 0$ for dry concrete.

***Second series of relations:***

$$f_{tdyn.} = f_{tsta.} + (6.57\ 10^{-4} \cdot M_{CSH} + 3.59\ g/g^{\star} - 2.79) \log(\dot{\sigma}_{dyn.}/\dot{\sigma}_{stat.}) \cdot \varphi(H) \quad (7)$$

where:

- $M_{CSH}$ is the massic content in CSH (in kg/m$^3$),
- $g/g^{\star}$ is the ratio of the actual aggregate proportion g to the ideal maximum proportion $g^{\star}$.

The first type of relations gives the average evolutions of the mechanical characteristics of concretes as a function of the loading rate, without taking into account the differences related to concrete mix design. These relations are linear functions of the logarithm of the loading rate, which is consistent with the fact that the jump of the concrete strengths, observed in the literature, is probably the result of a structural behaviour more than a material behaviour.

The second type of relations allows more precision and distinguishes between different concretes, taking into account some significant mix design parameters (F. Toutlemonde carried out a very complete and fine analysis to determine these significant mix design parameters [16]). No refined relation has been determined concerning the Young's modulus, which seems to show that the concrete mix design has a poor influence on the strain rate effect sensitivity of this mechanical characteristic [16]. Concerning the compressive strength, no relation is proposed due to the lack of experimental data.

## 4.2. Finite element constitutive relations

The LCPC uses two levels of modelling within the framework of a systematic strategy [17] to solve the practical problems. In this strategy, the two levels of modelling, considered as relevant at two scales of observation of concrete, are used to obtain different kinds of information:
– the first modelling level provides some relevant information for practical applications, as for example, the load capacity of the structure, the global displacements (deflection, ...), the parts of the structure where non-linearities appear;
– the second modelling level gives more precise information than the first. On the one hand, it permits a reliability analysis of the structure from the statistical results obtained on the load capacity and on the global displacements (using a Monte Carlo procedure), and on the other hand, it provides supplementary information on the basis of direct access to crack-patterns, crack-width, crack-spacing and failure mechanisms. Of course, this modelling level is also much more time-consuming.

Therefore, the choice of using one or two modelling levels will depend on the type (and the quality) of information required. For example, in the case where the information required leads to using the second modelling level, and where, in the structure studied, there are several non-linear zones due to its hyperstaticity, it is necessary to start with the first modelling level to determine the positions of these non-linear zones, which will then permit the optimization of the mesh using the second modelling level.

Before using non-linear models, it is always recommended to start with a linear elastic simulation: first, to determine the stress gradients in the structure, since the mesh elements of the non-linear simulation must be very small in relation to these gradients, and second, to evaluate the relevance of performing 2D non-linear simulations (which are, at the present, the more commonly used with non-linear models) by comparison with a 3D simulation (which gives the real stress fields).

The models being developed at the LCPC, within the framework of the proposed strategy to treat the dynamic behaviour of concrete structures, are an extension of static models validated and used to treat real civil engineering problems.

These models have been described in detail in Ulm [18], Rossi and Wu [19], Rossi and Ulm [20].

## 4.3 Static models

### *The plastic degrading model*

The purpose of the plastic degrading model is to model two apparent phenomena related to cracking: the permanent (or plastic) deformations and the irreversible degradation of elastic material properties (also designated as damage in the literature). With respect to standard coupled plastic-damage models (see, for instance, Lemaître and Chaboche [21]), where damage and plastic mechanisms are assumed to occur independently of each other, the plastic degrading model associates both phenomena with the same physical origin, *i.e.* cracking. More precisely, since the plastic variables, namely the plastic strain $\varepsilon^p$ and the hardening variables $\chi$, model the irreversible evolution associated with concrete cracking in a continuous manner, the damage associated with cracking necessarily coincides with the plastic evolution. For quasi-static evaluations and isotropic material behaviour, the following state equation is adopted :

$$\sigma = 2G(\chi)(e - e^p) + 3K(\chi)(\varepsilon - \varepsilon^p)1 \tag{8}$$

where $G(\chi)$ and $K(\chi)$ are the shear modulus and the bulk modulus, the evolution of which depend upon hardening variables $\chi$. Furthermore, $\varepsilon + e + \varepsilon 1$ and $\varepsilon^p = e^p + \varepsilon^p 1$ are the strain tensor and the plastic stain tensor (with $\varepsilon = tr\varepsilon/3$ and $\varepsilon^p = tr\varepsilon^p/3$). As in the standard plastic model, plastic evolution occurs when a loading point $\sigma$ is at the boundary of the elasticity domain $D_E$, defined by the loading function $f(\sigma,\zeta)$, thus:

$$\sigma \in D_E \Leftrightarrow f(\sigma,\zeta) \leq 0 \tag{9}$$

where $\zeta$ is the hardening force (current material threshold), which depends upon the hardening variable $\chi$ (*i.e.* $\zeta = \zeta(\chi)$). The evolution of hardening force $\zeta$ can be associated with the evolution of an energy *frozen* at the level of the heterogeneous material, which is not recovered as useful mechanical work upon unloading. More precisely, with respect to the heterogeneity of the matter, plastic evolution occurring during loading corresponds, at the level of the heterogeneous material, to a release of initial stresses, associated with an elastic energy *frozen* in the constituents. A part of this energy is dissipated by friction at the crack lips, while altering the initial stress state as well as the frozen energy. At the macroscopic level, the dissipation associated with friction phenomena is modelled in terms of plastic dissipation ($\sigma:d\varepsilon^p$ in time interval dt) reduced/increased by hardening/softening effects ($- dU = \zeta d\chi$). When neglecting second order strain terms in the state equations of a plastic degrading model, hardening force $\zeta$ derives from frozen energy U as in the standard plastic model

$$\zeta = \frac{-dU(\chi)}{d\chi} \tag{10}$$

A detailed discussion of this energy can be found in Coussy [22] and applied to concrete in Ulm [18]. Here, we note only that with respect to its origin, *i.e.* the material's heterogeneity, frozen energy U depends on the scale of observation of the material's heterogeneity, as well as

hardening force $\zeta$, and thus the threshold, *i.e.* when plastic evolution occurs. The evolutions of plastic variables $\varepsilon^p$ and $\chi$ are given by the flow and hardening rule:

$$d\varepsilon^p = d\lambda \frac{\partial g(\sigma,\zeta)}{\partial \sigma} \text{ and } d\chi = d\lambda \frac{\partial h(\sigma,\zeta)}{\partial \zeta} \quad (11)$$

where $d\lambda$ is the plastic multiplier, and $g(\sigma,\zeta)$ and $h(\sigma,\zeta)$ the plastic and hardening potential, defining the directions taken by plastic strain increments $d\varepsilon^p$ and hardening increments $d\chi$. Note clearly that hardening variable $\chi$ is a plastic variable (for instance, the plastic dilatation $\chi = \gamma^p_{eq} = \int 2d\mathbf{e}^p{:}d\mathbf{e}^p$, modelling the evolution of elasticity domain $D_E$ in state equation (9), as well as the evolution of elastic material properties $G(\chi)$ and $K(\chi)$ in state equation (7)). Plastic variable $\chi$ can thus be accessed - experimentally and numerically – independently of the degradation of elastic material properties. In other words, the information used (input) and requested (output) are on an equal basis, since they are measured/calculated independently of each other. Note, however, that plastic and hardening potentials $g(\sigma,\zeta)$ and $h(\sigma,\zeta)$, as well as plastic criterion $f(\sigma,\zeta)$, determined experimentally for concrete, are defined with respect to the scale of observation and will change, when passing from the scale that defines the representative elementary volume, where the model is designed to a lower modelling scale. To the knowledge of the authors, little attention has been paid to this fact in adaptive mesh strategies for elastoplastic problems.

The plastic degrading model is implemented in the finite element code CESAR-LCPC, and is accessible with different loading functions, plastic parameter Willam-Warnke criterion, with an associated rule ($g(\sigma,\zeta) = f(\sigma,\zeta)$). Strain-softening in the yield criterion is not considered (*i.e.* $dU/d\chi \geq 0$).

### *The discrete probabilistic cracking model*

Cracking of concrete is strongly influenced by the material's heterogeneity: the tensile strength of concrete is related mainly to that of the cement paste, which in turn is governed by the presence of voids, microcracks, etc. created during concrete hardening by non-uniform shrinkage during hydration at the scale of the heterogeneous material, *i.e.* at the scale of the concrete aggregates. This heterogeneity of the matter of which the concrete is made can be considered to be the basis for apparent size effects, governing the overall cracking behaviour at the macroscopic scale of material observation (*i.e.*, the scale of a laboratory test-specimen). This has led to the development of *the discrete probabilistic modelling of concrete cracking* over the last decade [19]. It belongs to the family of statistically-based deterministic models using the finite-element method. It accounts for cracks as geometrical discontinuities (discrete crack approach), and for the heterogeneity of the matter by random distribution functions with experimentally-determined mean values, $m(f_t)$ and $m(E)$, and standard deviations, $m(f_t)$ and $s(E)$, of tensile strength $f_t$ and Young's modulus E, respectively. For their experimental determination, major experimental research has been performed at the LCPC, which has led to the proposal of analytical expressions of the distribution functions (Rossi *et al.* [23]), based solely on the knowledge of:

1. the apparent compressive strength $f_c$ of the concrete, determined by a standardized test on a cylinder 16 cm in diameter and 32 cm high,
2. the ratio of the volume of concrete $V_t$ to the volume of the coarsest grain $V_g$.

In the finite-element analysis, these functions are used by replacing, in the experimentally determined distribution function, the volume of the test specimen $V_t$ by the volume of each solid finite-element. This is consistent with physical evidence: the smaller the scale of observation (the modelling scale) with respect to that of the structure, the larger the fluctuation of the local mechanical characteristics, and thus the (modelled) heterogeneity of the matter. This renders the numerical results mesh-independent (Rossi and Guerrier [24], and Rossi *et al.* [20]). As concerns the local and probabilistic character of the approach, the volume of the solid mesh elements must be sufficiently small with respect to the volume of the modelled structure, so that the probabilistic analysis performed on the scale of the mesh element is representative with respect to the structure.

The cracks are modelled using special contact elements that interface the solid elements. A crack (*i.e.* a contact element) "opens" (appearance of a geometrical discontinuity) when the stress normal to a fracture plane $\sigma_N = \mathbf{n}.\sigma.\mathbf{n}$ reaches the local tensile strength $f_t$, randomly distributed, thus:

$$\sigma_N - f_t \leq 0 \quad (12)$$

Crack criterion (1) refers to the fact that concrete cracking corresponds to a mode-I mechanism, in tension as well as in compression. In the latter, failure occurs due to the onset of oblique cracks (Torrenti *et al.* [25]). The failure mechanisms in compression and the consequences on the modelling scales are discussed in some detail in Rossi *et al.* [26]. The oblique cracks are created locally by tensile stresses. In order to capture this failure mechanism in terms of modelled heterogeneity, the modelling scale must be small with respect to the "structural" scale at which the failure occurs (small columns created by vertical cracks within the sample), and much smaller than that of the sample. At a higher scale, this oblique cracking appears as a shear failure and, within the limits of a homogeneous material, no tensile stresses occur in the material under compression (see Fig. 3). Hence, as concerns the modelled heterogeneity in the analysis, a shear-crack criterion may be necessary, expressed in its simplest form as:

$$|\tau| - c \leq 0 \quad (13)$$

where $\tau = \mathbf{t}.\sigma.\mathbf{n}$ is the shear stress and c is the local cohesion of the material. Since this crack-criterion reflects a mode-I criterion at a lower modelling scale, cohesion c cannot be regarded as an independent material characteristic – in contrast to the tensile strength $f_t$. In fact, since the oblique cracks open once the tensile stress reaches the local tensile strength, cohesion c is related to the tensile strength, so that:

$$c = \gamma f_t \quad (14)$$

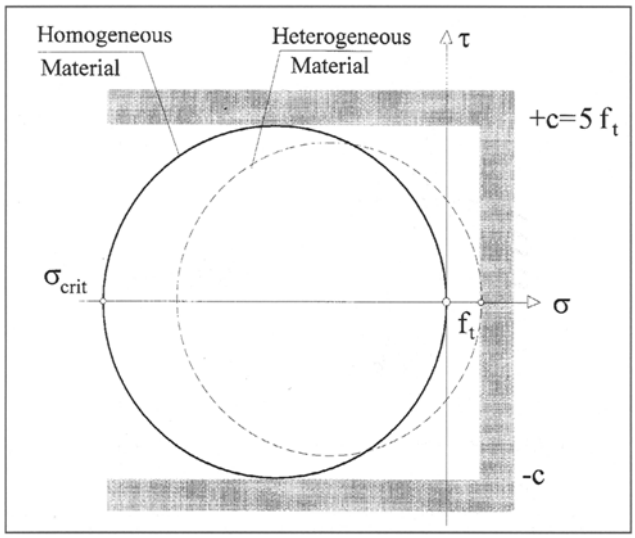


Fig. 3 – Mohr stress plane with different admissible stress states at different modelling scales of the heterogeneous material.

where $\gamma$ is a coefficient of proportionality, assumed constant. This assumption implies that the coefficient of proportionality is independent of size effects and allows for its determination from experimental data, ($\gamma = c / f_t \approx 5$, see Rossi *et al.* [26]). When a crack opens, local tensile strength $f_t$ and cohesion c are set to zero, and remain at zero throughout the calculation (local irreversible fragile tensile behaviour). In other words, the strength is not recovered when the crack recloses, and only normal compression stresses are admissible. The friction between the two edges of the geometrical discontinuity (edges of the crack) is taken into account by a cohesionless Mohr-Coulomb criterion reading:

$$|\tau| - \sigma_N \operatorname{tg}\varphi \leq 0 \tag{15}$$

With respect to the local irreverible fragile tensile behaviour, friction is only activated when the element recloses after opening. Note that an angle of friction $\varphi = 45°$ sufficiently represents the experimentally observed non-linear behaviour in the peak-load and post-peak load range in compression (Rossi *et al.* [23]).

## 4.4 Extensions of the models for dynamic loadings

### *The plastic degrading model*

The extension of the plastic degrading model in the dynamic field has been carried out by J. Sercombe *et al.* [27]. On the basis of the model in statics, a visco-elasto-plastic degrading model with viscous hardening has been developed.

The model being presented in detail in [27], we will focus here only on its main points.

In order to account for the rate dependency, a new material variable is introduced, x, which is related to viscous strain due to the Stéfan effect in the micropores of the concrete hydrates, giving:

$$d\varepsilon^v = B\, dx \tag{16}$$

$$dx/dt = A_x/\eta \tag{17}$$

where:
– $A_x$ is the associated force in the thermodynamic frame,
– $\eta$ is the viscosity associated with the viscous phenomenon.

The visco-elastoplastic degrading model with viscous hardening is illustrated in Fig. 4.

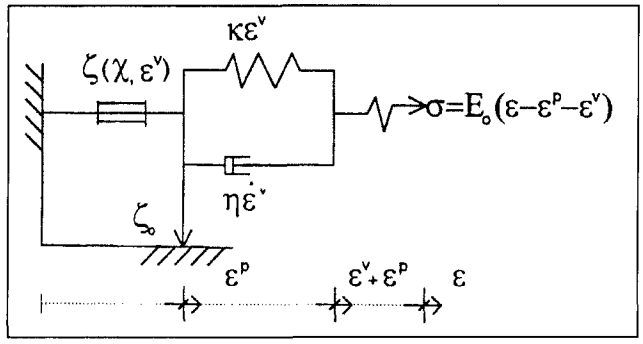


Fig. 4 – Visco-elastoplastic degrading model with viscous hardening.

In the model, the hardening force now also depends on the variable x or $\varepsilon^v$ (phenomenon of viscous hardening), as follows:

$$\zeta = \zeta(\chi) + \zeta(x) \tag{18}$$

with:

$$\zeta(x) = \frac{3{,}7\rho_0}{f_{tstat.}}\left\{1 - \frac{\log\left(\sqrt{3x}\right)}{\log\left[f_{tstat.}/k\right]}\right\} \tag{19}$$

This identification is consistent with relation (4).
$\rho_0$ is determined from Willam-Warnke criterion:

$$\tau + f(\theta)[p - \rho_0 + \zeta(\chi, x)] \leq 0 \tag{20}$$

where:
– p is the hydrostatic tenseur,
– $\tau$ is the second deviatoric invariant.

The 3D formulation of this model renders it consistent with relation (5).

### *The discrete probabilistic cracking model*

In [28], we proposed to replace, in relation (12), $f_t$ by $f_{tdyn}$ calculated using relation (2), $\sigma(f_t)$ being considered independent of the loading rate.

In fact, it appears that it is not a good way to take into account the strain rate effects in a material constitutive relation (for use in a finite-element analysis). Two main reasons support this remark:
– the first is a theoretical reason: it is not acceptable that a material's intrinsic characteristics be dependent on the loading rate,
– the second reason is related to numerical aspects: in a finite-element analysis, we cannot determine objectively, for a given time increment, the stress rate field.

R. Ben Romdhane [29], has recently returned to our first proposal, but in a better way, by using the same approach as J. Sercombe (in fact the two extensions were

initiated by O. Coussy and F. Ulm [30]). Thus, he proposes to replace, in relation (12), $f_t$ by $f_{tdyn}$, calculated using the following relation:

$$f_{tdyn.} = f_{tstat.} + \Delta f_t \quad (21)$$

with:

$$\Delta f_t = 3{,}7\left(\frac{\log X_c}{\log X_\infty} - 1\right) \quad (22)$$

$$x_c = \frac{f_{tstat.}}{k}\left\{1 - \frac{\eta\lambda}{f_{tstat.}k}\left[1 - \exp\left(-\frac{kf_{tstat.}}{\eta\lambda}\right)\right]\right\} \quad (23)$$

$$x_\infty = \frac{f_{tstat.}}{k} \quad (24)$$

where:
- $\eta$ is the viscosity associated to the viscous phenomenon (Stéfan effect),
- k is a rigidity parameter (see figure),
- $x_C$, and $x_\infty$ are related to viscous strains.

Thus, the elastic contact element used in the static calculation becomes a viscous contact element in the dynamic calculation, of which the rheological modelling is presented in Fig. 5.

The values of parameters k and h can easily be fitted to experimental data presented in Fig. 5.

Remark: It is obvious that the models developed at LCPC and presented above integrate the inertia effects necessary for a complete analysis of the dynamic structural behaviour.

## 5. RESEARCH WHICH REMAINS TO BE DONE

In view of the work already performed at LCPC, we can attempt to list what still needs to be analyzed concerning the behaviour of concrete structures submitted to dynamic loadings. Two main objectives appear as priorities:

1. The first objective is related to the validation or the determination of the domain of validity of the concrete models presented above. This can be realized by using these models to analyze the behaviour of full scale structural members subjected to realistic dynamic loadings. Verification of the experimental boundary conditions and of the loading are essential and unfortunately, there are not many experiments in the literature, except in [16], which respect these conditions.

2. The second objective is related to the mechanical behaviour and modelling of the interface between concrete and steel bars in reinforced concrete structures subjected to dynamic loadings. As a matter of fact, the behaviour of this interface plays a prominent part in the change of the mechanism of failure in reinforced concrete structures mentioned above. At present, the experimental results related to the dynamic behaviour of the rebar/concrete interface to be found in the literature are not numerous enough to develop an efficient model of this behaviour. So, this work remains to be done!

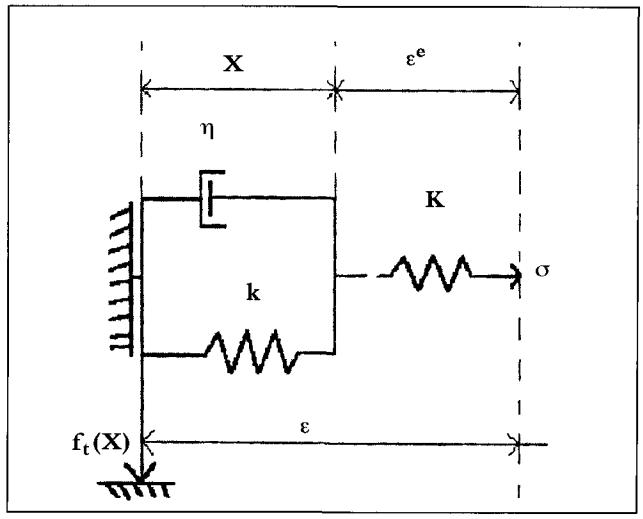

Fig. 5 – Rheological model of the viscous contact element.

Concerning the probabilistic discrete cracking model, we employ a special contact element to model the interface. Knowing that its behaviour strongly depends on the tensile behaviour of the concrete [14], we believe that a good solution would certainly be to develop a viscous contact element such as that developed for the discrete concrete cracking model. The parameters of the constitutive equation related to this viscous element could be determined by using relations similar to relation (4).

## 6. CONCLUSIONS

We have presented in this paper the research strategy the LCPC has chosen to analyze the dynamic behaviour of concrete structures. This strategy is based upon three steps:
- *Step 1*: Understanding the physical mechanisms at the origin of rate effects in concrete by performing a large number of experimental tests at the material level.
- *Step 2*: Developing mechanical models which are physically relevant for design code and finite-element analysis.
- *Step 3*: Validating the models by simulating tests on full scale structural members.

The physical mechanisms that may be involved in the dynamic behaviour of concrete in tension, and which may explain the loading rate effects observed experimentally, can be summed up as follows:

1. At strain rates smaller than approximately 1 $s^{-1}$, the main physical mechanism is a viscous mechanism that may be regarded as similar to the Stéfan effect. This mechanism opposes both microcracking localization, leading to an increase of tensile strength (behaviour at the material level), and the macrocrack propagation that leads to failure of the specimen (structural behaviour).

2. At strain rates greater than or equal to approximately 10 $s^{-1}$, the forces of inertia become preponderant. Like the Stéfan effect, these forces oppose microcracking localization and macrocrack propagation. The increase of tensile strength observed at these rates is perhaps not

intrinsic to the material, since the forces of inertia, which are very large in the stage of macrocrack propagation, can lead to an increase of the maximum load even after microcracking localization. This would be a structural effect and would have to be taken into account as such in any mechanical and numerical modelling.

3. The viscous effects, together with the forces of inertia, result in an increase of the Young's modulus of the concrete, but to a much smaller extent than the tensile strength, because as far as Young's modulus is concerned, the aggregates, which play a major role, are not sensitive to the viscous effects.

Taking into account these physical mechanisms, two types of models have been developed to perform finite-element analysis of concrete structures:
– the first model provides some relevant information for pratical applications, for example, the load capacity of the structure, the global displacements (deflection, ...), the parts of the structure where non-linearities appear. This is a *visco-elastoplastic degrading model with viscous hardening*;
– the second model provides more precise information than the first, because, on one hand it permits a reliability analysis of the structure from the statistical results obtained on the load capacity and on the global displacements (using a Monte Carlo procedure) and, on the other hand, it provides supplementary information on the basis of direct access to crack-patterns, crack-width, crack-spacing and failure mechanisms (rigid motions, for example); of course, it is also much more time-consuming. This is a *probabilistic discrete viscous cracking model.*

The two models are being implemented in the LCPC finite-element code CESAR-LCPC.

Their validation remains to be done.

Finally, to analyze the dynamic behaviour of reinforced concrete structures, it is necessary to use the same three-step strategy for modelling the rebars/concrete interface as for concrete. This work also remains to be done.

## 7. REFERENCES


[1] Rossi, P., 'A physical phenomenon which can explain the mechanical behaviour of concrete under high strain rates', *Mater. Struct.* **24** (1991) 422-424.

[2] Rossi, P., Van Mier, J. M. G., Boulay, C. and Le Maou, F.,'The dynamic behaviour of concrete: influence of free water', *Ibid.* **25** (1992) 509-514.

[3] Rossi, P., Van Mier, J. M. G., Toutlemonde, F., Le Maou, F. and Boulay, C., 'Effect of loading rate on the mechanical behaviour of concrete subjected to uniaxial tension', *Ibid.* **27** (1994) 260-264.

[4] Rossi, P., 'Dynamic behaviour of concrete: from the material to the structure', *Ibid.* **27** (1994) 319-323

[5] Toutlemonde, F., Boulay, C. and Gourraud, C., 'Shock-tube tests of concrete slabs', *Ibid.* **26** (1993) 38-42.

[6] Toutlemonde, F., Rossi, P., Boulay, C., Gourraud, C. and Guédon, D., 'Dynamic behaviour of concrete: tests of slabs with a shock tube', *Ibid.* **28** (1995) 293-298.

[7] Toutlemonde, F. and Rossi, P.,'High-strain rate tensile behaviour of concrete: significant parameters', in 'Fracture Mechanics of Concrete Structures', edited by F. H. Wittmann (Aedificatio 1995) vol. I, 709-718.

[8] Toutlemonde, F. and Rossi, P., 'Shock-tested R.C. slabs: significant parameters', A.S.C.E. Structure Congress XII, Atlanta, edited by N.C Baker and B.J. Goodno, Vol. 1 (1994) 227-232.

[9] Toutlemonde, F. and Rossi, P., 'Are high-performance concretes (HPC) suitable in case of high rate dynamic loading?', 4th International Symposium on Utilization of High Strength/High-Performance Concrete, Paris, edited by F. de Larrard and R. Lacroix (1996) 695-704.

[10] Rossi, P. and Toutlemonde, F., 'Effect of loading rate on the tensile behaviour of concrete: description of the physical mechanisms', *Mater. Struct.* **29** (186) (1996) 116-118.

[11] Acker, P., Boulay, C. and Rossi, P., 'On the influence of initial stresses in concrete and the resulting mechanical effects', *Cement and Concrete Research* **17** (1987) 755-764.

[12] Rossi, P. and Wu, X., 'A probabilistic model for material behaviour analysis and appraisement of concrete structures', *Magazine of Concrete Research* **44** (161) (1992) 271-280.

[13] Bailly, P., 'Une modélisation d'un matériau fragile avec prise en compte d'effets dynamiques', Comptes Rendus de l'Académie des Sciences, Paris, T. 318, série II (1994) 1-6 (in French).

[14] Reinhardt, H.W., 'Concrete under impact loading. Tensile strength and bond', *Heron* **27** (3) (1982) Delft.

[15] Weerheijm, J., 'Concrete under impact tensile loading and lateral compression', PhD Thesis, T.U. Delft (1992).

[16] Toutlemonde, F., 'Résistance au choc des structures en béton: du comportement du matériau au comportement de structure', LCPC research report (1995, in French).

[17] Rossi, P. and Ulm, F., 'A strategy for analyzing the mechanical behaviour of concrete structures under various loading: the LCPC experience' in 'Fracture Mechanics of Concrete Structures', edited by F. H. Wittmann (Aedificatio 1995) Vol. II, 1271-1284.

[18] Ulm, F., 'Modélisation élastoplastique avec endommagement du béton de structure. Application aux calculs statiques et dynamiques des structures en béton armé et béton précontraint', PhD thesis from École Nationale des Ponts et Chaussées, Paris, (1994, in French).

[19] Rossi, P., and Wu, X., 'A probabilistic model for material behaviour analysis and appraisement of the concrete structures', *Cement and Concrete Research* **44** (161) 1992 271-280.

[20] Rossi, P., Ulm, F., 'Sizes effects in biaxial tensile-compressive behaviour of concrete: physical mechanisms and modelling', in 'Fracture Mechanics of Concrete Structures', edited by F. H. Wittmann (Aedificatio 1995) Vol. I, 543-556.

[21] Lemaitre, J. and Chaboche, J.L., 'Mechanics of Solid Materials', (Cambridge University Press, 1990).

[22] Coussy, O., 'Mechanics of porous media' (John Wiley & Sons, Chichester, England, 1995).

[23] Rossi, P., Wu, X., Le Maou, F., and Belloc, A., 'Scale effect on concrete in tension', *Mater. Struct.* **27** (1994) 437-444.

[24] Rossi, P. and Guerrier, F., 'Application of a probabilistic discrete cracking model for concrete structures', in 'Fracture and Damage in Quasibrittle Structures: Experiment, Modelling and Computer Analysis', edited by Z.P. Bažant *et al.* (E. & F.N. Spon 1994) 303-309.

[25] Torrenti, J.M., Benaija, E.H. and Boulay, C., 'Influence of boundary conditions on strain softening in concrete compression test', *J. of Engng. Mech., ASCE* **119** (12) (1993) 2369-2384.

[26] Rossi, P., Ulm, F., and Hachi, F., 'Compressive behaviour of concrete: physical mechanisms and modelling'. Accepted for publication in ASCE Engineering Mechanics.

[27] Sercombe, J., Ulm, F. and Toutlemonde F., 'Modelling of concrete in high rate dynamics', in 'Structural Dynamics Eurodyn'96', edited by G. Augusti, C. Borri & P. Spinell (A.A. Balkema 1996) Vol. I, 481-488.

[28] Rossi, P., 'Comportement dynamique des structures en béton: du matériau à la structure', *Annales de l'ITBTP* **511** (1993) 27-38.

[29] Ben Romdhane, R., 'Élaboration d'un modèle visqueux d'interface au comportement dynamique pour le module PROB CESAR-LCPC', DEA from École Nationale des Ponts et Chaussées, Paris (1995 in French).

[30] Coussy, O. and Ulm, F., 'Creep and plasticity due to chemo-mechanical coupling', *Archive of Applied Mechanics* **66** (1996), Spring Velag, 1-13.